ROYAL SOCIETY OPEN SCIENCE

royalsocietypublishing.org/journal/rsos

Research

Cite this article: Shabangu FW, Yemane D, Stander N, Estabrook BJ. 2025 Underwater soundscape indicates low anthropogenic influence around two sub-Antarctic islands. *R. Soc. Open Sci.* **12**: 250677.
https://doi.org/10.1098/rsos.250677

Received: 8 April 2025
Accepted: 22 October 2025

Subject Category:
Ecology, conservation, and global change biology

Subject Areas:
ecology, ecosystem, acoustics

Keywords:
anthropogenic footprint, acoustic ecology, environmental conditions, noise pollution, passive acoustic monitoring

Author for correspondence:
Fannie W. Shabangu
e-mail: fannie.shabangu@yahoo.com

Supplementary material is available online at https://doi.org/10.6084/m9.figshare.c.8151827.

THE ROYAL SOCIETY PUBLISHING

Underwater soundscape indicates low anthropogenic influence around two sub-Antarctic islands

Fannie W. Shabangu[1,2], Dawit Yemane[1], Nicky Stander[3] and Bobbi J. Estabrook[4]

[1]Fisheries Management Branch, Department of Forestry, Fisheries, and the Environment, Foreshore, Cape Town 8001, South Africa
[2]Mammal Research Institute Whale Unit, Faculty of Natural and Agricultural Sciences, University of Pretoria, Hatfield, Pretoria 0028, South Africa
[3]Southern African Foundation for the Conservation of Coastal Birds, Cape Town 7441, South Africa
[4]K. Lisa Yang Center for Conservation Bioacoustics, Cornell Lab of Ornithology, Cornell University, Ithaca, NY 14850, USA

FWS, 0000-0002-3668-3566; DY, 0000-0001-7293-2534; BJE, 0000-0002-5639-899X

Contributions and effects of anthropogenic activities on the underwater soundscape of the sub-Antarctic regions remain poorly studied. Over a 21-month period (April 2021 to December 2022), we recorded underwater noise levels amid two sub-Antarctic Prince Edward Islands (PEIs) within an offshore marine protected area with the aim to quantitatively investigate the sources of underwater noise and the impact of such noise on the detectability of marine mammal vocalizations. We measured underwater noise levels within the low (20–120 and 121–800 Hz), medium (801–25 000 Hz) and high (25 001–48 000 Hz) frequency bands. Wind speed was the primary predictor of low and medium frequency underwater noise levels, whereas iceberg volume was the primary predictor at the high frequency band. Probabilities of detecting vocalizations of Antarctic blue, fin, humpback, Antarctic minke and killer whales decreased with increasing noise levels. On the contrary, probabilities of detecting sei and Madagascan pygmy blue whale vocalizations increased with noise levels. Overall, these novel results indicate that geophonic noise dominates the underwater soundscape of the PEIs in the absence of intense anthropogenic activities such as marine traffic, and that the detectability of marine mammal underwater vocalizations is species-specific.

1. Introduction

Underwater passive acoustic monitoring is a powerful, non-lethal and non-invasive tool for investigating relationships between marine organisms and their underwater environment, including anthropogenic activities. To naturally achieve the above goal, information from *in situ* passive acoustic research is required to provide representative and defensible estimates of underwater sound levels and indications of how marine organisms respond to those sound levels [1–5]. Acoustic modelling can be used in the absence of *in situ* acoustic data, but this does not always represent actual acoustic conditions [6]. Underwater sounds are generated by three sources: anthrophony (e.g. sounds from vessel traffic, sonar, wind energy, and operations related to gas and oil exploration), geophony (e.g. sounds from wind and wave actions, rain, sea ice, volcanoes and earthquakes) and biophony (e.g. sounds from marine mammals, molluscs, crustaceans and fish) [4,7,8]. A combination of ambient sounds (which might include anthrophony, geophony and/or biophony) over frequency, time and space is termed soundscape [9]. Specifically, this study refers to distal soundscape which is defined by Grinfeder *et al*. [9] as 'the spatial and temporal distribution of sounds in a prespecified area, in relation to sound propagation effects'.

Marine mammals and other marine organisms need suitable areas with relatively good quality soundscapes in order for them to perform important biological processes. For example, marine mammals utilize sound to communicate with conspecifics at long ranges and under low-light conditions [10,11], to echolocate [12], to find mates [13,14], to fight off mating competitors [13,14], to avoid ship strike [3] and to avoid predators [12]. Elevated underwater noise levels can have varying effects on marine organisms' behaviour, including inducing avoidance from the sound source [15], stop feeding [12], increase their sound level to counter the increasing noise level, i.e. Lombard response [16], or they may become habituated [17]. In extreme cases, hearing loss [1] and even death can occur [1,3]. Thus, it is imperative to understand the role of underwater noise in the context of the acoustic environment of various species in order for us to implement conservation practices, policies, regulations, mitigation measures and management strategies that will protect or reduce impacts of at-sea human activities on these animals [1,3,4].

The Prince Edward Islands (PEIs) marine protected area (MPA) was declared in 2013 [18] and was established with the sole intention to significantly contribute towards global initiatives to protect and conserve offshore and deep ocean areas from anthropogenic activities. The PEIs are located in the sub-Antarctic, Indian Ocean sector of the Southern Ocean and are approximately 2000 km southeast of Cape Town, South Africa, and 2300 km from Antarctica (figure 1). South Africa has been the sovereign state of these islands since 1948, and the PEIs MPA represents South Africa's first offshore MPA. The PEIs MPA is a multi-use zone MPA that consists of a sanctuary zone, four restricted zones and controlled zones between restricted zones (figure 1) [20]. Due to their remoteness and isolation, the PEIs represent one of the few remaining near-pristine sub-Antarctic regions. The close proximity of the PEIs to the biologically productive sub-Antarctic Front and Antarctic Polar Front [21] makes these islands important breeding and feeding area for seabirds, seals and killer whales [22,23] and a relevant habitat for baleen whales [24].

Following that there is only one study [25] measuring underwater noise levels in the sub-Antarctic region (off Crozet Island and Kerguelen Plateau), a big knowledge gap on underwater noise levels and their impacts on marine organisms exists in this important area of the Southern Ocean. Therefore, the objectives of this study were to (i) measure the PEIs' underwater noise levels, (ii) determine sources of underwater noise and their contribution to the soundscape of the PEIs, and (iii) determine how the acoustic detectability of marine mammals is influenced by noise level variabilities.

2. Material and methods

2.1. Collection of passive acoustic data and whale presence determination

Passive acoustic data were collected between two sub-Antarctic islands, Marion Island and Prince Edward Island, Southern Ocean (figure 1), from April 2021 through May 2023 (table 1). A SoundTrap ST500 STD acoustic recorder manufactured by Ocean Instruments NZ, New Zealand, was installed on an oceanographic mooring (details of the oceanographic mooring setup are provided in Shabangu *et al* [24]). The acoustic recorder was serviced and redeployed once per year. The SoundTrap was set to sample for 14 min on half the hour of every hour of each day to avoid interference with the

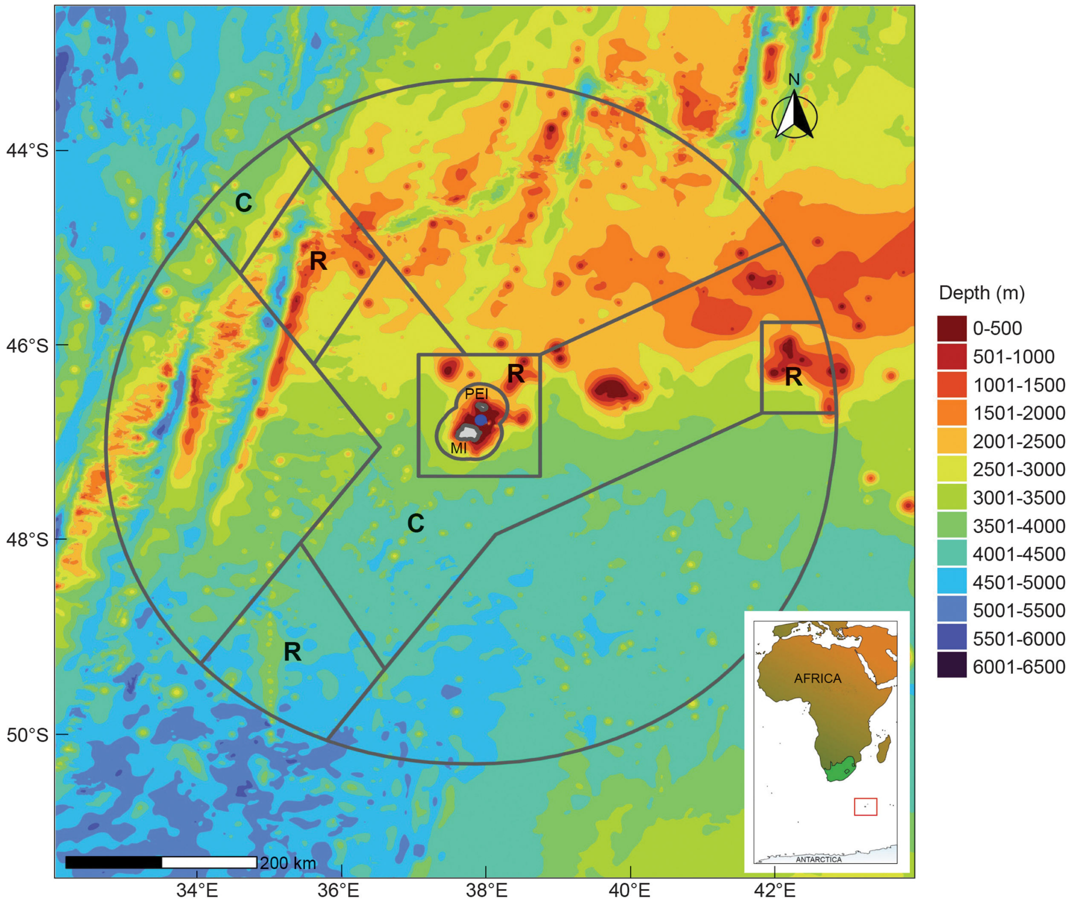

Figure 1. The position of Prince Edward Islands (PEIs) in the Southern Ocean showing the bigger Marion Island (MI) and smaller Prince Edward Island (PEI), the PEIs' exclusive economic zone (big open circle), marine protected area (MPA) zones (divisions within the circle) and 12 nautical mile territory waters (figure-of-eight polygon) around the PEIs. Within internal divisions, C indicates the controlled zones and R indicates restricted zones. Position of the oceanographic mooring with the acoustic recorder is indicated by closed blue circle between PEI and MI. Inset map shows the position of the PEIs (small red box) in relation to South Africa's mainland (green shading in the African map) and Antarctica. Bathymetry data were downloaded from General Bathymetric Chart of the Oceans (GEBCO) [19].

acoustic Doppler current profiler (ADCP) that sampled on the clock of every hour. We used hourly occurrence (i.e. presence/absence) of seven marine mammal species from two previous studies [23,24] to define acoustic detectability of marine mammals around the PEIs. Acoustic detectability refers to the probability of marine mammal vocalizations to be detected under various noise levels at the acoustic receiver location. The seven marine mammals studied here are Antarctic blue (*Balaenoptera musculus intermedia*), Madagascan pygmy blue (*B. m. brevicauda*; mainly found across the southwestern Indian Ocean), Antarctic minke (*B. bonaerensis*), Southern Hemisphere fin (*B. physalus*), sei (*B. borealis*), humpback (*Megaptera novaeangliae*) and killer (*Orcinus orca*) whales. As reported in Shabangu *et al.* [23,24], the following vocalization types are used in this study to represent different behavioural states of marine mammals: Z-calls for Antarctic blue whale communication; D-calls for blue whale foraging; unit 1 and 2 of Madagascan pygmy blue whale calls for communication; fin whale 20 Hz pulses for communication; fin whale 40 Hz pulses for foraging; Antarctic minke whale bioduck calls for communication; sei whale upsweep calls for communication; humpback whale songs for communication; killer whale social calls for communication; killer whale echolocation clicks for foraging and navigation.

2.2. Oceanographic data

The below oceanographic variables were considered to determine the effect of oceanographic conditions on levels of ambient noise around the PEIs. Oceanographic conditions data were extracted from a 2° (222 km latitude) × 2° (156 km longitude) quadrant centred over the mooring location.

Table 1. Passive acoustic data collection details including the SoundTrap (ST) autonomous acoustic recorder settings. Sensitivity value is from factory calibrations of the HTI-96-MIN (High Tech Inc.) hydrophone.

latitude (°S)	longitude (°E)	water depth (m)	ST depth (m)	sampling rate (kHz)	sampling protocol (min h^{-1})	duty cycle (%)	hydro-phone sensitivity (dB re 1 V μPa^{-1})	start recording date (dd/mm/yyyy)	end recording date (dd/mm/yyyy)
46.77	37.91	167	162	96	14	23	−165	26/04/2021	06/05/2022
46.77	37.91	165	160	96	14	23	−165	09/05/2022	26/04/2023

This spatial resolution was used because some of the satellite-derived and reanalysis oceanographic variables, particularly total precipitation and wind speed, were only available at a 0.25° (28 km) spatial resolution which is too coarse to detect fine local shelf dynamics to avoid land contamination [26]. Furthermore, there is a good correlation between *in situ* data from Marion Island and 2° × 2° block [27], which makes these satellite-derived and reanalysis data indicative of the environment around the PEIs. Ocean current speed was measured locally via an ADCP deployed on the mooring. All the oceanographic data listed below were read and analysed using 'raster' [28] and 'tidyverse' [29] packages in R statistical software [30].

2.2.1. Wind and precipitation

Meridional (v) and zonal (u) wind speeds (m s^{-1}) and total precipitation (m) provided on an hourly scale by the fifth generation of European Centre for Medium-Range Weather Forecasts (ECMWF) reanalyses (ERA5) [31] were downloaded from https://cds.climate.copernicus.eu/cdsapp#!/dataset/reanalysis-era5-single-levels?tab=form. Total precipitation consists of accumulated liquid and frozen water from rain and snow that falls to the ocean's surface, and a spatial resolution of 0.25° × 0.25° was used to collect the obtained data [31]. Global grids with 0.25° × 0.25° spatial resolution at 10 m above the surface of the Earth were used to collect the ERA5 wind speed data [31]. Absolute wind speed and wind direction were calculated from u and v vectors as follows:

$$ws = \sqrt{u^2 + v^2}, \tag{2.1}$$

$$wdt = atan2\left(\frac{u}{ws}, \frac{v}{ws}\right), \tag{2.2}$$

$$wdd = wdt \times 180/\pi, \tag{2.3}$$

$$wdn = wdd + 180, \tag{2.4}$$

where ws is the absolute wind speed, u is zonal wind speed, v is meridional wind speed, wdt is wind direction trigonometry, wdd is wind direction trigonometry to degrees and wdn is meteorological wind direction angle (degrees north).

2.2.2. Ocean waves

Hourly significant height of combined wind waves and swell (m; henceforth wave height) and peak wave period (s; henceforth wave period) data sampled at 0.5° × 0.5° spatial resolution were obtained from ERA5. Wave height indicates the at-sea observed total wave field formed by combining shorter wind waves that are influenced by wind and longer swell waves produced by distant winds and waves moving across the ocean basins. Wave period represents the time when the majority of the wave energy is concentrated. Wave period was used for this study to determine the amount of noise generated by breaking waves as they interact with the seabed.

2.2.3. Iceberg volume

Icebergs generate distinct loud underwater sounds as their volumes change due to various physical processes such as movement, grinding, crunching, shattering, cracking and melting [7,8]. To capture the influence of iceberg volume change on the PEIs' soundscape, we used level 3 merged Antarctic polar stereographic bi-weekly iceberg (less than 3 km in length) volume (total gigatons (Gt)) data. These iceberg volume data sampled at 50 km resolution grids were obtained from the Centre de Recherche et d'Exploitation Satellitaire (CERSAT), at IFREMER, Plouzané (France), Altiberg database [32]: ftp://ftp.ifremer.fr/ifremer/cersat/projects/altiberg/v3.2/data/antarctic/merged/grid/2-weekly/50km/polar-stereographic/netcdf. We extracted the data between 20° and 60° E (i.e. 20° flanking the PEIs) and calculated the total bi-weekly iceberg volume by summing the corresponding data from all grid cells from Antarctica to the PEIs. The European Petroleum Survey Group (EPSG) projection code for converting polar stereographic projection to project into the Southern Hemisphere Projection geographic coordinate system was obtained from https://nsidc.org/data/user-resources/help-center/guide-nsidcs-polar-stereographic-projection.

2.2.4. Current speed data collection

Hourly speeds of ocean current (cm s^{-1}) were used as frontal activities proxy around the mooring location, and these were collected by an upward looking Teledyne RDI 150 kHz QuarterMaster ADCP that was suspended 5 m off the sea bottom on the oceanographic mooring [33,34]. Ocean current speed data were collected on the clock of every hour, and these were used to represent the hourly current speed. ADCP current speeds were measured throughout the water column (18.88–150.96 m); however, we considered only hourly values with ≥75% good beam data, and data from the ADCP beam closer to the acoustic recorder's depth.

2.3. Vessel traffic

Maritime traffic from fishing, supply, research and tourism vessels exposes the most isolated and remote sub-Antarctic regions to human impacts. Hourly vessel traffic data derived from automatic identification system (AIS), which is used to track ships, were attained from Clarksons Platou (H. Clarksons & Company Limited). These AIS data contained information on the date, hour, number of vessels, unique ID number for each vessel, vessel speed over ground, vessel type and distance of vessels from acoustic station within four sections (described below) around the PEIs identified from acoustic propagation modelling of baleen whale calls (electronic supplementary material, figure S1) [24]. Hourly vessel traffic information for statistical data analysis was extracted to a maximum distance of 53 km (and then weighted below according to the four sections), a distance after which vessel traffic contribution to the local soundscape becomes negligible [5]. The 53 km range also corresponds to the Madagascan pygmy blue whale maximum detection range of 53 km around the PEIs in summer, autumn and winter [24]. To account for acoustic shadowing by the PEIs as found by Shabangu *et al.* [24], four azimuthal sections were created around the PEIs where section 3 was largely blocked by Marion Island (electronic supplementary material, figure S1) and had an average maximum detection range of 10 km. As a result, vessel traffic from sections 1, 2 and 4 were weighted more to 53 km than those from section 3 that were weighted to 10 km.

To estimate monthly vessel traffic around the PEIs, the AIS data were processed to the spring average maximum detection range of Antarctic blue whale Z-call of 730 km [24]. To determine the distance of AIS tracked vessels from the acoustic recorder location, monthly unweighted number of vessels was calculated at different distance categories: 0–5, 6–10, 11–20, 21–50, 51–110, 111–200, 201–500 and 501–730 km. Due to the sparsity of vessel presence within the 53 km grid, data on weighted vessel speed over ground, vessel type and distance of vessels from acoustic station were available for 5% h and 7% days of the whole study period. Therefore, weighted vessel speed over ground, vessel type and distance of vessels from acoustic station were excluded from further analysis while hours without information for number of vessels were filled with zeros to represent absence of vessels.

2.4. Estimation of noise levels

Passive acoustic data analysis to estimate noise levels around the PEIs was performed using a custom MATLAB program [35]. To capture the contribution of different sound sources to the underwater soundscape of the PEIs, noise levels were measured within four frequency bands: 20–120, 121–800, 801–25 000 and 25 001–48 000 Hz. These frequency bands represent low (20–120 and 121–800 Hz), medium (801–25 000 Hz) and high (25 001–48 000 Hz) frequency groups. We did not consider data below 20 Hz for our analysis due to high internal acoustic recorder noise below that frequency. To calculate noise levels, acoustic data were processed using a Hann window with zero overlap (to simplify calculations and reduce computational load), and a fast Fourier transform with 1 s and 1 Hz resolution. Equivalent continuous sound pressure level (L_{eq}), in dB re 1 μPa, is the average sound level over a specified period. L_{eq} is used in this study to represent the average unweighted sound pressure of a continuous time-varying signal, with an averaging time of 14 min to represent noise levels for the hour in which the data were collected. L_{eq} can also be used to represent the sound energy that can potentially cause hearing damage to marine mammals due to cumulative exposure. Noise statistics are visually represented using long-term spectrograms, 1/3-octave spectrograms, root-mean-square sound pressure level (SPL_{RMS}) and percentiles of power spectral density (PSD) plots. Broadband noise from the SoundTrap calibration tone (approx. 2.75 s long) at the beginning of every recording and ADCP tones (occurring every 72 s and about 1 s in duration; examples of these ADCP tones are given in fig. 2 of Shabangu *et al.* [24]) were removed from the processed data using a custom function in R. Acoustic data from January to April 2023 were found to be contaminated by high (>110–150 dB re 1 μPa SPL) wideband internal noise (electronic supplementary material, figures S2 and S3) from the hydrophone (John Atkins, Ocean Instruments), and such data were excluded from further noise data analysis. Consequently, acoustic occurrence data from April 2021 to May 2022 and April 2021 to December 2022 were used for killer whales [23] and baleen whales [24], respectively.

2.5. Quantitative data analysis

The influence of oceanographic conditions on the ambient L_{eq} around the PEIs was evaluated using random forest (RF) models [36]. As a machine learning technique, RF models allow for non-parametric inferences; inherent inclusion of interactions among predictors; reasonably good predictive performance; and return estimated variable importance as part of model fits and they can handle large and small sample sizes with high dimensional data [36,37]. Vessel traffic was the least important variable across all four frequency bands; this might have to do largely with the low vessel traffic within 53 km around the PEIs (see §3.1). Thus, it was excluded from the below final model. The results from the initial model that included vessel effect are presented in complementary RF model results presented in the electronic supplementary material. Final RF models for modelling predictors of ambient noise levels (L_{eq}) at different frequency bands were fitted using equation (2.5):

$$L_{eq} \sim m + h + ws + wd + tp + wh + wp + wad + ibv + cs, \tag{2.5}$$

where m is month, h is hour in Universal Coordinated Time zone, ws is wind speed, wd is wind direction, tp is total precipitation, wh is wave height, wp is wave period, wad is wave direction, ibv is iceberg volume and cs is current speed.

The influence of ambient L_{eq} on the acoustic detectability (affected by masking, whale vocalizing behavioural change and distance of vocalizing whales to acoustic recorder) of six baleen whale species (Antarctic blue, Madagascan pygmy blue, fin, Antarctic minke, sei and humpback whales) and one dolphin species (killer whales) was modelled using generalized linear model (GLM) regression [38]. GLM allows, through the use of link function, to model response variable generated by multiple generating processes (e.g. binomial distribution) that will represent the number of successes in a fixed number of independent trials, each with the same probability of success. GLM also allows count processes other than a Gaussian processes and expresses the relationship as a linear function/combination of all the predictors. The underlying relationship between predictor and response variables is assumed by this model to be linear; however, nonlinearity can be explicitly specified in multiple ways including polynomial function and B-spline. To get rid of the previously observed correlation between frequency bands [5], the low (20–120 Hz) and high (25 001–48 000 Hz) frequency bands were used to model the acoustic detectability of marine mammals. Probability of detecting marine mammal vocalizations at the recording location was quantified at different L_{eq} to a point of 0.5 at which a species probability of detection would decrease or increase considerably. The GLMs for marine mammal detectability were fitted using equation (2.6):

$$SD \sim LFB + HFB, \tag{2.6}$$

where SD is species detectability, LFB is low frequency band and HFB is high frequency band.

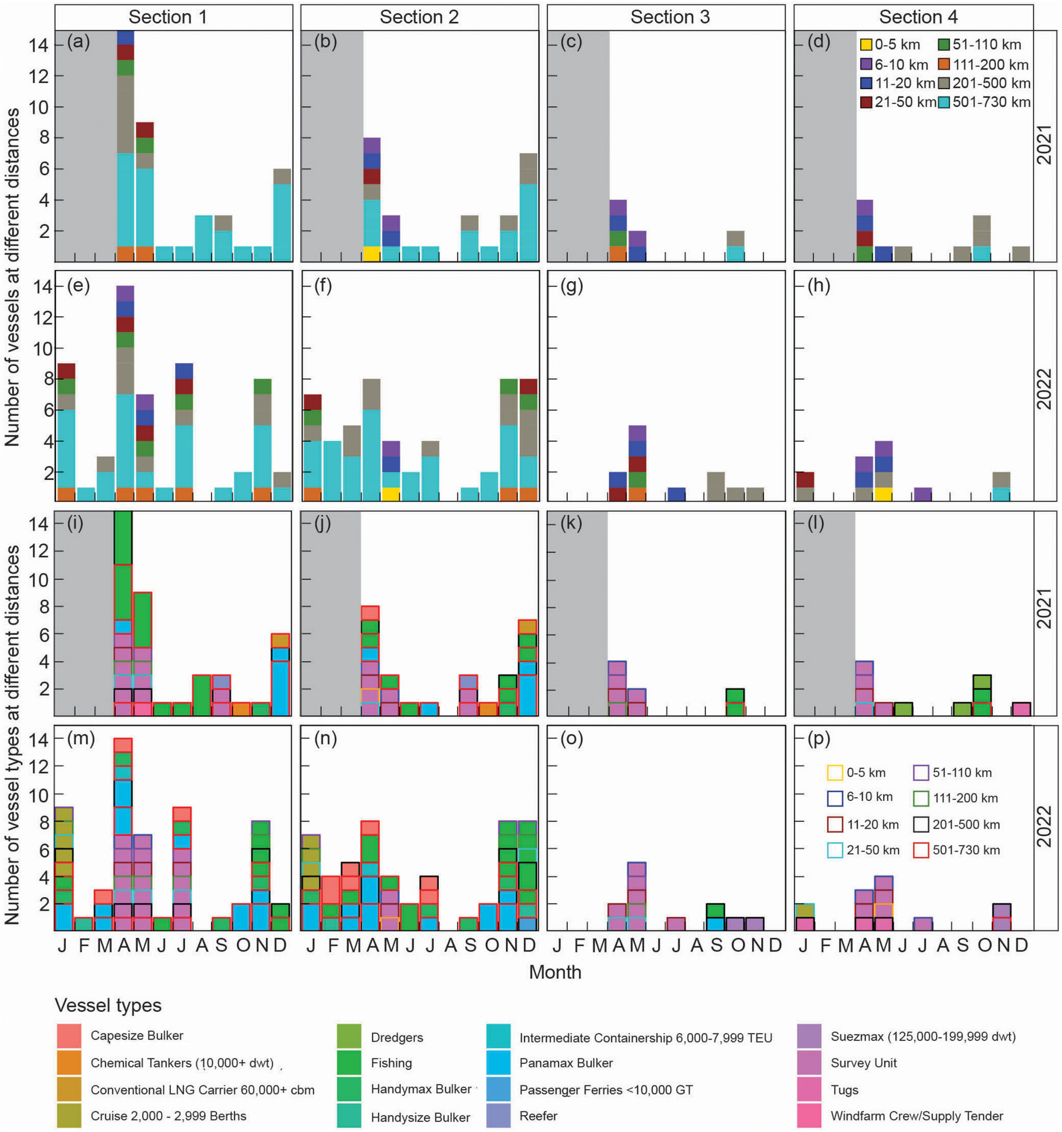

Figure 2. Sectional (a–h) unweighted number of vessels tracked at different distances from the acoustic recorder location, and (i–p) number of each vessel type tracked at different distances from the acoustic recorder location derived from automatic identification system (AIS) data for April 2021 to December 2022. Key for distance colours for (a–h) is in (d), distance colour key for (i–p) barplot borderlines is in (p), and key for vessel type is provided in the bottom panel.

2.5.1. Tuning and testing models

Before modelling the influence of oceanographic variables on ambient L_{eq} at different frequencies and the influence of ambient L_{eq} on acoustic marine mammal detectability, variance inflation factors (VIFs) were determined among predictor variables and no to low multicollinearities were found as the highest VIF value was 2.17. Four different methods to account for clear class imbalance of marine mammal acoustic occurrence were used: adaptive synthetic (ADASYN) [39], downsampling and upsampling [40] and synthetic minority over-sampling technique (SMOTE) [41]. All sample balancing methods were used because all sample balancing methods performed similarly, and none was better than the other (electronic supplementary material, figure S4). For training, 70% of the sample balanced data were used for tuning all models and the remaining 30% were used for testing. The rest of the tuning and testing were performed using the same method as that described in Shabangu *et al.* [5].

2.5.2. Relative importance

Improvement response variance and the firm approach [42,43] were used to evaluate the relative importance of predictor variables for RF models and GLMs respectively. Partial effect relative flatness of a variable measured the variables' importance for the GLMs. For each model, feature importance of all variables was scaled to the maximum and outputted as percentage. Each feature importance value significance (*p*-value) was checked using the Altmann *et al.* [44] permutation method to enable straightforward interpretation of our RF model results. The 'randomForest' package [45] was used to perform the above RF modelling, and the RF model tuning was implemented through the 'ranger' package [46] in R. GLMs were fitted using the 'tidymodels' R package [47]. The 'tidyverse' R package was used to process, analyse, visualize and summarize all data and results.

3. Results

3.1. Vessel traffic around Prince Edward Islands

The AIS data revealed that a total of 58 unique vessels were present within the maximum range of 730 km over the 21 months (for 601 days or 3401 h), and only three vessels were found within the 53 km sector (figure 2a–h). Of the three vessels found within 53 km, one was a survey unit (South African icebreaking polar supply and research ship, *SA Agulhas II*) in April and May of 2021 (for 11 days) and 2022 (for 26 days), one was a cruise liner (MSC *Orchestra*) with 2000–2999 berths in January 2022 (for 1 day), and the other was a fishing vessel found for 5 days in November and December 2022 (figure 2). Most of the vessel traffic were detected from section 1 and 2 (figure 2) that face the South African and Australian mainland (electronic supplementary material, figure S1). April had the highest vessel traffic per distance category for all sections over the study period, and a total of 31 vessels over various distances was the highest number of vessels found in April 2021 (figure 2). April also corresponds to the time when the *SA Agulhas II* travels to the PEIs for scientific crew changeover and provide supplies to the research station at Marion Island and also to conduct research around the PEIs.

In 2022, January, July, November and December had the second highest vessel traffic for section 1 and 2 (figure 2a,b,e,f). Fishing vessels were the dominant vessel type within the 730 km sector but were mostly more than 200 km from the acoustic recorder location (figure 2i–o). However, a fishing vessel was found within 53 km distance from the acoustic recorder location on three occasions in November and December 2022 (figure 2m,n). Only one survey unit, *SA Agulhas II*, moved as close as 0.1 km to the acoustic recorder location (figure 2j,n) to recover and redeploy the oceanographic mooring.

3.2. Underwater noise and oceanographic conditions trends

For all frequency bands, there were small increases in ambient L_{eq} from February 2022 through August 2022 with minor decreases in L_{eq} thereafter (figure 3a). Median L_{eq} was around 98 dB re 1 μPa for all frequency bands. The high frequency band (25 001–48 000 Hz) had the lowest noise levels, whereas the medium (801–25 000 Hz) band had the highest noise level. For brevity's sake, only oceanographic conditions that were found to be significantly important in §3.3 are presented here. Daily wind speeds were high in the austral winter and spring but low in austral summer and autumn (figure 3b). Bi-weekly iceberg volume increased from early August to early February and then decreased until the end of July. Wave height was low in summer and high in winter (figure 3b). No seismic survey signals were detected in these data; however, earthquake sounds were detected sporadically. There was a constant band of noise in the low frequency band (figure 4a,b). SPL_{RMS} noise was higher for the low frequency band than for the high frequency band and was mostly below 120 dB re 1 μPa (figure 4c). PSD percentile plots over the deployment period show sound pressure spectrum levels without distinct peaks below 150 Hz but with some intermittent peaks above 200 Hz (figure 4d). Significant PSD variabilities (10–30 dB re 1 $\mu Pa^2\ Hz^{-1}$) between the 5th and 95th percentiles were visible.

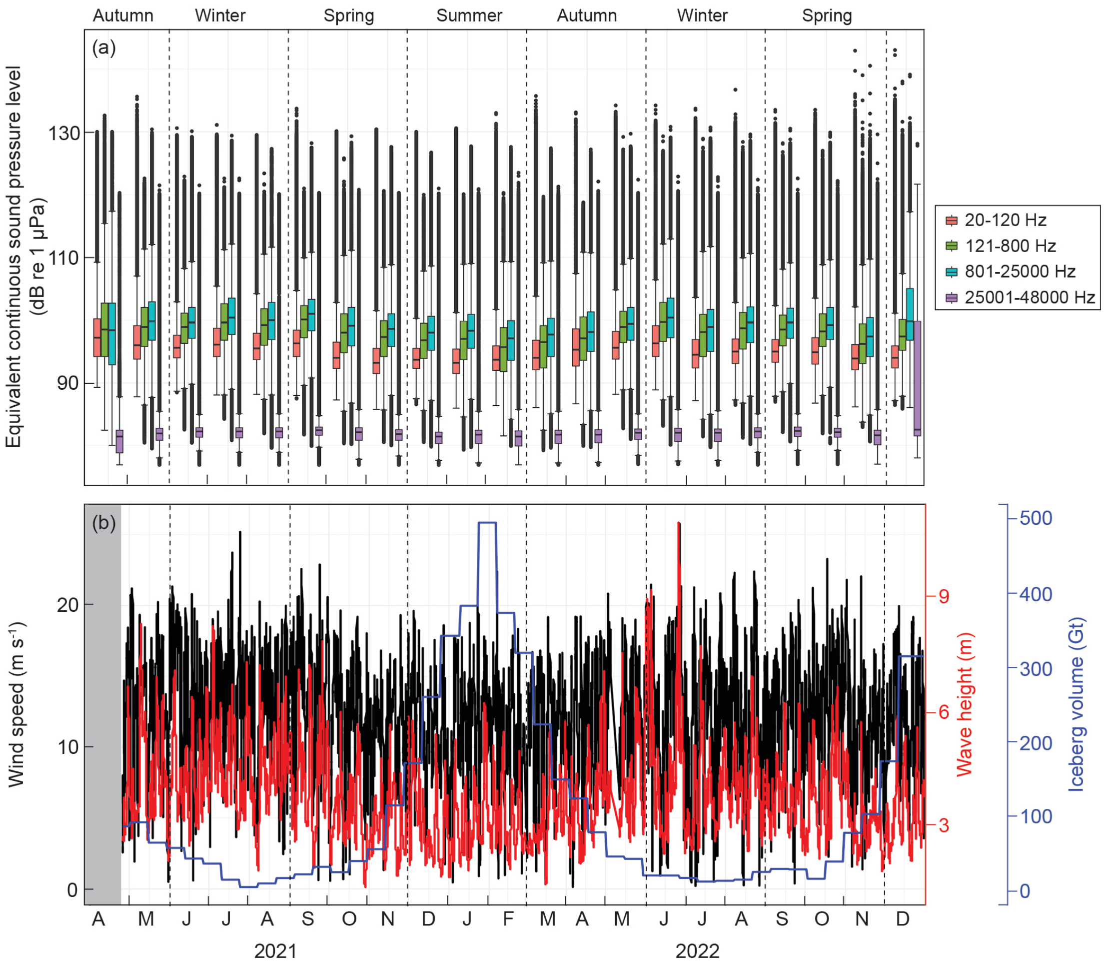

Figure 3. (a) Monthly box and whisker plots of L_{eq} (equivalent continuous sound pressure level) at different frequency bands, and (b) daily wind speed, daily wave height and bi-weekly iceberg volume (colour coded). Boxes in (a) show the interquartile range from the first to the third quartile, black horizontal lines inside boxes represent medians, closed circles represent L_{eq} values that are outside the range covered by whiskers, and whiskers indicate 1.50 times the interquartile width. Months are abbreviated on the *x*-axis. December through February represent summer, March through May represent autumn, June through August represent winter, and September through October represent spring.

3.3. Ambient noise predictors

The RF models indicated no notable change in ambient noise levels (L_{eq}) for all frequency bands relative to current speed and hour of day (figure 5a). The L_{eq} for the 25 001–48 000 Hz frequency band increased with iceberg volume between 298 and 330 Gt and plateaued thereafter; however, there were minor iceberg volume influences on other frequency bands. For the 20–120 Hz frequency band, influence of month on L_{eq} increased from January to April and then decreased at varying rates until December. Slight increase in noise levels was observed in December for the 25 001–48 000 Hz frequency band (figure 5a). Minor influences of total precipitation on noise levels were found for the low and medium frequency bands. A >2 dB re 1 μPa^2 Hz^{-1} noise increase was observed for the 25 001–48 000 Hz frequency band when total precipitation increased from 0 to 0.0018 m.

Wave direction between 240° and 360° slightly influenced noise level increase for all frequency bands (figure 5a). Noise levels increased with wave height for the 20–120, 121–800 and 801–25 000 Hz frequency bands; however, for the 25 001–48 000 Hz frequency band, noise levels increased with wave height up to 3 m and decreased thereafter. There were minor L_{eq} increases with increasing weighted total number of vessels for all frequency bands (electronic supplementary material, figure S5). Noise levels decreased with increasing wave period up to 15 s and showed little difference to 17.5 s for the 20–120, 121–800 and 801–25 000 Hz frequency bands (figure 5a). No changes were observed for the 25 001–48 000 Hz frequency band relative to wave period. Noise levels fluctuated with changing wind direction and did not show any pattern for all frequency bands. L_{eq} for the 20–120, 121–800 and 801–25

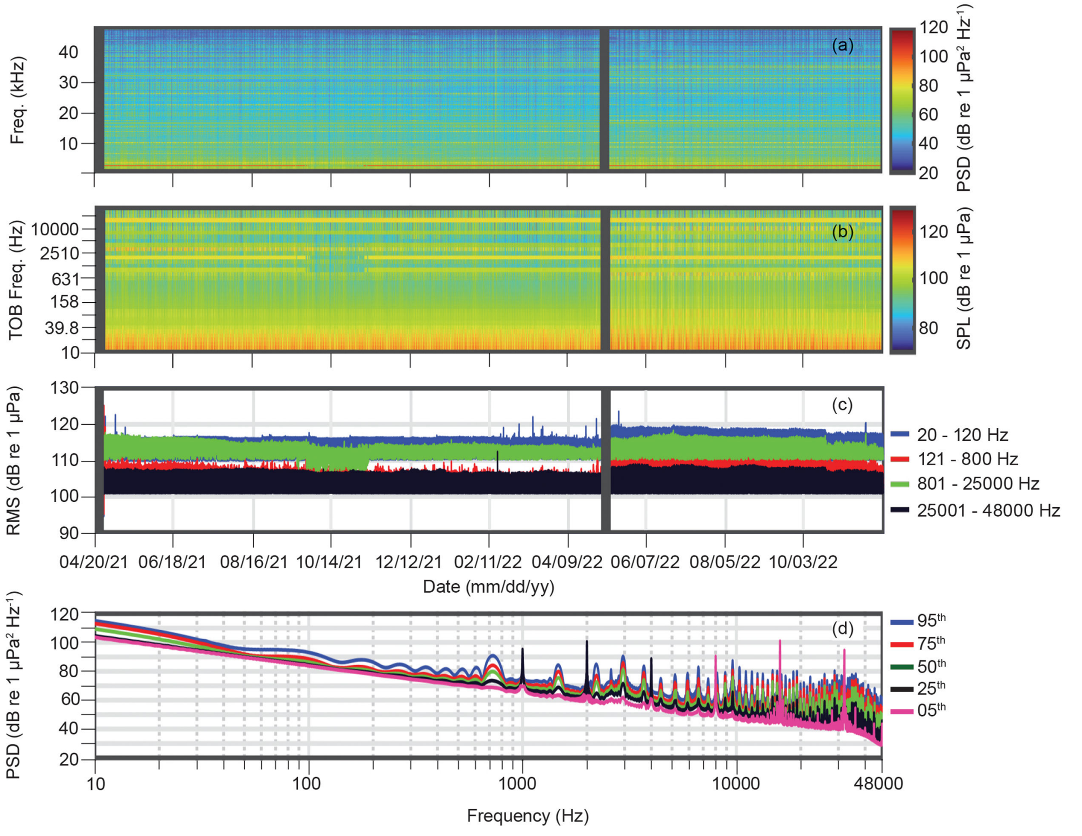

Figure 4. (a) Long-term spectrogram, (b) 1/3-octave band (TOB) spectrogram, (c) root mean square (RMS) sound pressure level (SPL_{RMS}) at different frequency bands and (d) percentiles of power spectral density (PSD) for April 2021 through December 2022 period. Dark grey vertical lines in (a–c) represent periods without acoustics data. Freq. is for frequency.

000 Hz frequency bands increased with wind speed to a maximum of 25 m s^{-1}, while L_{eq} for the 25 001–48 000 Hz frequency band increased with wind speed to 15 m s^{-1} and decreased after that (figure 5a).

Wind speed was the most important predictor of noise levels for the 20–120, 121–800 and 801–25 000 Hz frequency bands, whereas iceberg volume was the most important predictor of noise levels for the 25 001–48 000 Hz frequency band (figure 5b). Wave height was a moderately important predictor for the 20–120, 121–800 and 801–25 000 Hz frequency bands noise levels, whilst wind speed, wave direction and month were the moderately important predictors of noise levels in the 25 001–4 80 000 Hz frequency band. Other remaining variables were the least important predictors of ambient noise levels. Wind speed, wave height, iceberg volume and month were significant and informative predictors of noise levels in the 20–120 Hz frequency band. Wind speed and wave height were significantly important predictors of noise levels in the 121–800 Hz frequency band (figure 5b). Only wind speed and wave height were the significantly important predictors of noise levels in the 801–25 000 Hz frequency band. For the 25 001–48 000 Hz frequency band, iceberg volume and month were the only significantly important predictors of underwater noise levels (figure 5b).

3.4. Whale vocalizations and ambient noise

From different sample balancing methods, probabilities of detecting Antarctic blue whale Z-calls, blue whale D-calls, fin whale 20 and 40 Hz pulses, humpback whale songs, Antarctic minke whale bioduck calls, killer whale social calls and echolocation clicks decreased with increasing ambient noise levels in the 20–120 Hz frequency band except for Madagascan pygmy blue and sei whale calls, which increased with ambient noise levels (figure 6). Noise levels in the 25 001–48 000 Hz frequency band did not influence the detectability of the Antarctic blue whale Z-calls (figure 6a). Probabilities of detecting blue whale D-calls, Madagascan pygmy blue whale calls, fin whale 20 Hz pulses, Antarctic minke whale bioduck calls, killer whale social calls and echolocation clicks decreased with increased noise

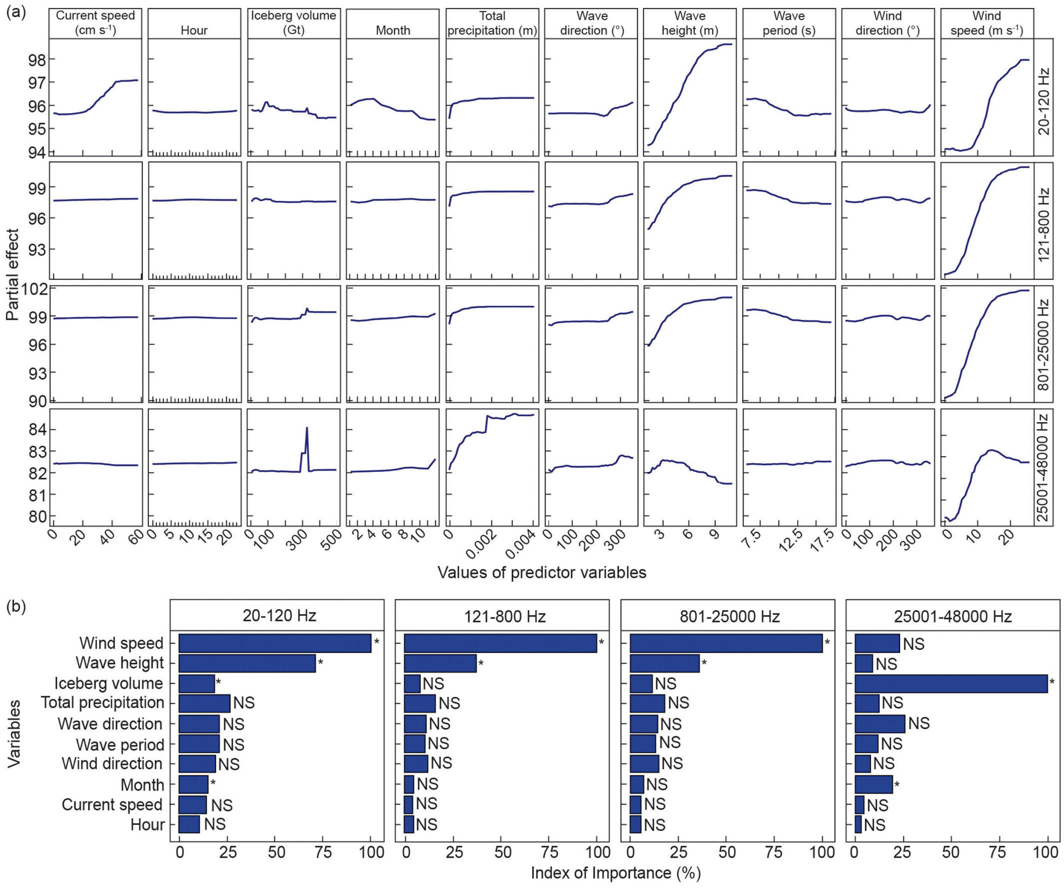

Figure 5. RF (random forest) model (a) partial effect and (b) ranked importance of predictor variables on the ambient L_{eq} (equivalent continuous sound pressure level) at different frequency bands. Asterisks indicate significantly important variables, and NS indicates non-significantly important variables.

levels in the 25 001–48 000 Hz frequency band (figure 6b,c,d,g,i,j). By contrast, probabilities of detecting fin whale 40 Hz pulses, humpback whale songs, and sei whale upsweep calls increased with noise levels in the 25 001–48 000 Hz frequency band (figure 6e,f,h). About 90% of acoustic detectability of Antarctic blue whales, blue whale D-calls, fin whale 20 and 40 Hz pulses, humpback whales, Antarctic minke whales, killer whale social calls and echolocation clicks was below the 50% point in the 20–120 Hz frequency band (figure 6a,b,d,e,f,g,i,j). Approximately 80% of acoustic detectability of Madagascan pygmy blue and sei whales was above the 50% point in the 20–120 Hz frequency band (figure 6c,h). For killer whales, 80% of their acoustic detectability was below the 50% threshold for both the 20–120 and 25 001–48 000 Hz frequency band noise but decreased at a faster rate for the 25 001–48 000 Hz frequency band than for the 20–120 Hz frequency band (figure 6i,j). The 50% point was passed at slightly high ambient noise levels around 98 dB re 1 μPa at the low frequency band but at a lower noise level around 80 dB re 1 μPa at the high frequency bands for all marine mammals (figure 6).

4. Discussion

This study provides the first quantitative and detailed description of the underwater soundscape of the PEIs. Results of this study show that the soundscape of the PEIs at 20–120 to 801–25 000 Hz frequency bands is dominated by geophonic noise from wind speed, and the 25 001–48 000 Hz frequency band soundscape is predicted by iceberg volume. Very few vessels were found within 53 km radius around the PEIs on a seasonal basis, and their presence significantly contributed to the area soundscape. The detectability of the focal marine mammal signals varied with underwater noise levels in the low and high frequency bands in a species-specific manner.

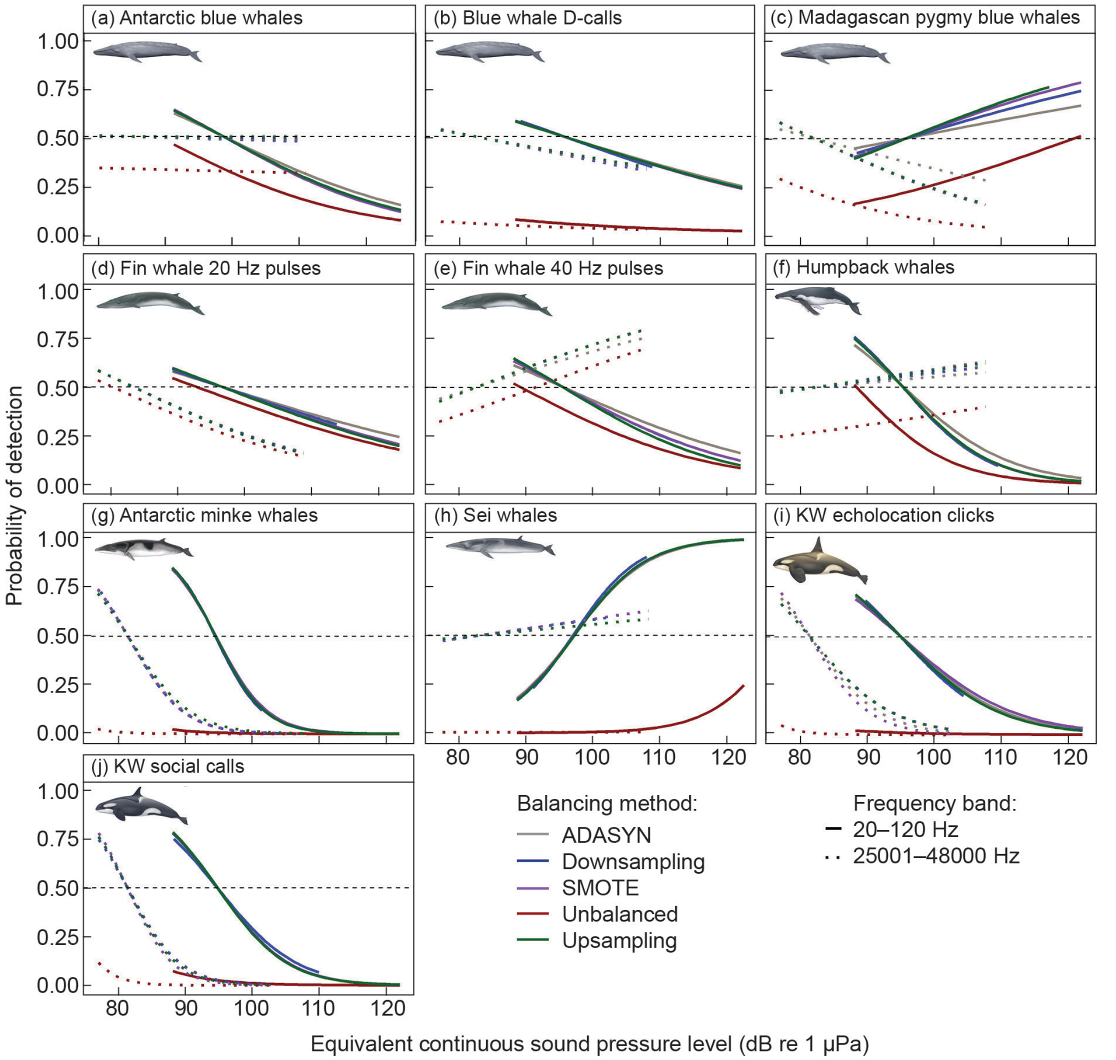

Figure 6. (a–j) GLM (generalized linear model) dose–response curves of ambient L_{eq} (equivalent continuous sound pressure level) partial effect on the probability of detecting marine mammals acoustically at the low (continuous lines) and high (dashed lines) frequency bands for each marine mammal species according to different sample balancing methods. KW is for killer whale. The 50% point for acoustic detection of marine mammals at a given noise level is represented by the dashed horizontal line at 0.5.

4.1. Vessel traffic trend

The maximum of 31 vessels found in April 2021 within 730 km around the relatively pristine PEIs is considerably lower than vessel traffic of up to 5000 or so vessels per month observed off the west coast of South Africa [5]. Very few vessels transited through the PEIs on the way to Antarctica; however, such ship traffic in the Southern Ocean might introduce invasive species to these remote and isolated areas [48]. The *SA Agulhas II* was the only vessel that moved very close to the acoustic recorder location, an encouraging sign that vessel traffic is very low in this region. However, the presence of a fishing vessel within the 53 km sector from the acoustic recorder is concerning as this might be indicative of illegal fishing [49] within the PEIs MPA if the vessel was not transiting through the area. The second highest vessel presence for section 1 in July 2022 was due to the *SA Agulhas II* having to go to the PEIs for a medical emergency. Observed increase in vessel traffic in January, November and December for sections 1 and 2 corresponds to the austral summer movement of vessels to and from Antarctica. Vessel traffic estimates presented in this study are likely conservative since AIS tracking is known to sometimes underestimated vessel traffic especially for fishing vessels that interfere or turn off their AIS transponders [50].

4.2. Underwater soundscape predictors

Noise levels in this sub-Antarctic region did show minor monthly and seasonal patterns (figures 3 and 4), which is contrary to huge seasonal noise variations in the Antarctic [8,51,52]. The observed little seasonal noise variation could be due to the PEIs being an open water environment year-round and does not have sea ice cover that seasonally limits wind- and wave-induced underwater noise and limits vessel traffic in some seasons. Whale vocalizing activities around the PEIs were not detected at loud enough levels to increase sound levels above the ambient noise (figure 4), which is different from Antarctica where baleen whales and geophonic noise equally contributed to the Antarctic soundscape [8,52,53]. The received low contribution of marine mammal sounds to the PEIs soundscape may be due to masking from strong geophonic noise in the low and medium frequency bands [5,7]. Alternatively, this could be due to relatively fewer vocalizations detected in the low/mid latitudes compared with Antarctica [51,54,55].

Hydrophone flow noise was not a problem for these acoustic recordings given the minor contribution (approx. 1.4 dB re 1 μPa) of current speed to the sound level, which is different from results from the west coast of South Africa where comparable current speed created high flow noise contamination [5]. The observed differences in flow noise between the two regions might be due to differences in water depth where hydrophones were deployed and designs of acoustic recorders (SoundTrap versus AURAL-M2) since current speeds are comparable between the two regions—hence, this topic requires more special investigation. Time of day was not influential on ambient noise as there were no diel variations of main noise producers. Contrary to previous studies [8,25,52,56], the influence of iceberg volume on the low frequency noise (20–120 Hz) for this study decreased with increase in iceberg volume which signifies that iceberg volume does not dominate the low frequency soundscape of this open water region. However, iceberg volume had a high and significant influence on the 25 001–48 000 Hz frequency band when the volume was between 298 and 330 Gt, suggesting that iceberg volume can contribute to higher frequency noise level as documented for ice noise by Wenz [7]. Additionally, this result suggests that ice cracking noise is audible around the PEIs at greater distances from the sea ice edge in Antarctica as observed by Tsang-Hin-Sun *et al.* [25]—although small icebergs are sometimes observed floating pass the PEIs.

The high influence of January to April for the 20–120 Hz frequency band coincided with the observed change in iceberg volume (figure 3), and the April increase in vessel presence around the PEIs from the *SA Agulhas II* since that is the frequency band dominated by vessel noise [5,7]. December had the greatest influence on underwater noise from the 801–25 000 and 25 001–48 000 Hz frequency bands since this is the month that iceberg volume started to peak (figure 3). Total precipitation had the highest influence on the noise levels in the 25 001–48 000 Hz frequency band, since precipitation sounds are prominent in that frequency band [7]. The rapid increase of ambient noise at the first increase of total precipitation was also observed off the west coast of South Africa [5].

Wave direction from the northwest (between 240° and 360°) resulted in increased noise levels at all frequency bands as water would have been channelled between the PEIs in line with the northward movement of the sub-Antarctic Front [23]. Noise levels decreased at all frequency bands with an increase in wave period as observed off the west coast of South Africa [5] since sound intensity decreases with increased wave period [57]. No pattern of wind direction influence was discernible at all frequency bands, confirming that direction of wind does not influence underwater noise levels [5]. The observed increase in ambient noise levels with wind speed is due to wind-induced sea surface turbulence and agitation that generate underwater noise at wide frequencies [58]. Air bubbles entrapped in the shallow water layer during sea wave action produce underwater noise as bubbles dilate and burst due to pressure changes associated with surface water movement induced by the wind [58]. Wave height showed similar influence (to that of wind speed) on the PEIs' soundscape due to high positive correlation between the two variables [59]. The dome shaped influence of wave height and wind speed on the high frequency band (25 001–48 000 Hz) indicates dissipation of noise from these two variables at high frequency.

Wind speed was the most important predictor of ambient noise for the 20–120, 121–800 and 801–25 000 Hz frequency bands, indicating that wind speed dominated the soundscape of this region in the absence of anthropogenic activities such as shipping [60]. For example, vessel noise dominated the low frequency (10–500 Hz) in areas with high vessel traffic, such as the west coast of South Africa [5]. Iceberg volume was the most important predictor of ambient noise for the 25 001–48 000 Hz frequency band, which supports the finding of Wenz [7] that ice can contribute to noise higher than 10 kHz. Moderately and least important predictors contributed to the ambient noise but not as high as the most important predictors. Ambient noise can be informatively predicted by significantly important predictor variables, while ambient noise cannot be informatively predicted by all predictor variables with non-significant importance. Thus, iceberg volume was informative at predicting low frequency noise (20–120 Hz frequency band) even though it does not dominate the ambient noise at that frequency band.

Previous open ocean noise studies in the sub-Antarctic region [25] and Antarctica [8,52,53,56,61] did not consider vessel traffic as a potential source of underwater noise of those regions as they presumed that low vessel traffic did not contribute or contributed negligibly to ambient noise. However, our results demonstrate that the low vessel traffic does significantly contribute to the soundscape of these regions (electronic supplementary material, figure S5) at least on a seasonal basis when vessels are very close to the recorder location. Hence, vessel noise contributes to the soundscape of these regions at least on a seasonal basis when ships visit the sub-Antarctic (this study) and Antarctic regions [62]. This study's approach of considering multiple variables analysed through RF models with implicit interaction implemented between predictor variables allowed for a holistic and quantitative understanding of the multiple predictors of ambient noise and drivers of the soundscape dynamics around the PEIs. Overall, the remoteness and protected state of the PEIs might be maintaining the soundscape of this region near-pristine with little anthropogenic influence.

4.3. Marine mammals and ambient noise

The detectability of Antarctic blue and fin whales around the PEIs decreased with increasing noise at both the low and high frequency bands, reflecting masking of whale vocalizations by ambient noise produced by geophonic sources (mainly wind speed). The acoustic detectability of Antarctic blue and fin whales shows a different pattern from that observed off the west coast of South Africa where their detectability increased with increasing underwater noise that was largely dominated by vessel noise [5]. Detectability of blue whale foraging and mating call, D-call, also decreased with increasing noise levels—a further testament that geophonic noise reduced the detectability of whale calls. Contrary to Antarctic blue and fin whales, Madagascan pygmy blue whale acoustic detectability increased with increasing noise in the low frequency band, perhaps demonstrating their acoustic behavioural adaptation to the windy environment in their native southern Indian Ocean region [63] of Madagascar. Furthermore, this increased detectability with increasing noise levels could indicate that Madagascan pygmy blue whales were closer to the acoustic recorder location to enable call detection above the ambient noise level. Decreased acoustic detectability of other whale vocalizations with increasing noise could indicate that vocalizing whales were distant, masking of calls by noise [2] and attenuation of the focal signals by wind-induced air bubbles on the shallow surface layer [58,64]. Both masking and attenuation reduce marine mammal communication spaces and propagation ranges of marine mammal sounds.

Probability of detecting Antarctic minke and humpback whales also decreased with increasing noise level from the low frequency band, which is similar to results found off the west coast of South Africa [5]. Just like off the west coast of South Africa, humpback whales had higher detectability when the high frequency band noise (dominated by ice volume induced noise for this region) was high, perhaps demonstrating a Lombard response. Likewise, humpback whales off eastern Australia showed a Lombard response to wind noise but not to vessel noise [16]. Sei whales' detectability increased with noise levels in both the low and high frequency bands, indicating that vocalizing whales could have been much closer to the PEIs for calls to have higher signal strength above the level of ambient noise. Alternatively, these sei whales could be exhibiting a Lombard response to increasing noise. Killer whale acoustic detectability for both social calls and echolocation clicks decreased with increasing ambient noise levels, indicating that this killer whale population does not acoustically counteract geophonic originating underwater noise. The reduced detectability of killer whale vocalizations likely resulted in shortened communication ranges of these animals.

5. Conclusion

Here, we provide the first measurements and description of predictors of underwater noise around the PEIs, and first indication of how the acoustic detectabilities of six baleen whale species and one delphinid species are influenced by ambient noise levels in this sub-Antarctic region. Geophonic noise from wind speed and iceberg volume dominated the soundscape around the PEIs; however, vessel noise significantly influenced the soundscape when vessels (mainly a research vessel) were seasonally present in the area. Vessel traffic around the PEIs was very low, and no other anthropogenic activities contributed to the underwater soundscape, which qualifies this area as near-pristine from vessel noise. Continuation of this passive acoustic monitoring research is critical and fundamental at establishing long-term changes in the ecosystem and conservation efforts of some of the endangered species in the Southern Hemisphere. To conclude, it is encouraging that this region is less influenced by anthropogenic activities in the Anthropocene era, and marine mammals are still safe from anthropogenic noise when in this region. However, special noise management and mitigation measures are required for this critical region to keep anthropogenic noise low. Novel results of this study advocate for continued protection and strengthened management to protect this important region and its biodiversity from emerging threats and stressors. Lastly, this study provides baseline noise level measurements for this PEIs MPA which is important for the conservation of the marine mammals studied here and for future noise monitoring and management in this region.

Ethics. Acoustic data collection on the oceanographic mooring was carried out under a permit from the Director-General: Department of Forestry, Fisheries and the Environment, South Africa.

Data accessibility. Data are provided in the form of an RData file containing noise levels at different frequency bands, acoustic occurrence of all marine mammal vocalizations, vessel traffic and environmental data [65]. Links for accessing environmental data are provided in §2.2.

Electronic supplementary material is available online [66].

Declaration of AI use. We have not used AI-assisted technologies in creating this article.

Authors' contributions. F.W.S.: conceptualization, data curation, formal analysis, funding acquisition, investigation, methodology, project administration, resources, supervision, visualization, writing—original draft, writing—review and editing; D.Y.: data curation, formal analysis, software, writing—review and editing; N.S.: data curation, methodology, writing—review and editing; B.J.E.: conceptualization, data curation, formal analysis, methodology, software, visualization, writing—review and editing.

All authors gave final approval for publication and agreed to be held accountable for the work performed therein.

Conflict of interest declaration. We declare we have no competing interests.

Funding. This work was supported by the International Whaling Commission, the South African Department of Forestry, Fisheries and the Environment, and the South African National Research Foundation.

Acknowledgements. The International Whaling Commission is acknowledged for funding the purchase of the acoustic recorder used in this study. Many thanks to Clarksons Platou (H. Clarksons & Company Limited) for kindly providing the AIS data. We thank the captains and crew of the SA Agulhas II as well as staff (particularly Dr Tarron Lamont and Mr Marcel van den Berg) and affiliated students from the South African Department of Forestry, Fisheries and the Environment for their professional assistance with the deployment and retrieval of the oceanographic mooring and acoustic data thereof. F.W.S. is grateful to SMRU Consulting, UK, for travel support. Many thanks to Uko Gorter for generously providing whale illustrations.

References

1. Southall BL *et al*. 2008 Marine mammal noise-exposure criteria: initial scientific recommendations. *Bioacoustics* **17**, 273–275. (doi:10.1080/09524622.2008.9753846)
2. Clark C, Ellison W, Southall B, Hatch L, Van Parijs S, Frankel A, Ponirakis D. 2009 Acoustic masking in marine ecosystems: intuitions, analysis, and implication. *Mar. Ecol. Prog. Ser*. **395**, 201–222. (doi:10.3354/meps08402)
3. Erbe C, Marley SA, Schoeman RP, Smith JN, Trigg LE, Embling CB. 2019 The effects of ship noise on marine mammals—a review. *Front. Mar. Sci*. **6**, 606. (doi:10.3389/fmars.2019.00606)
4. Duarte CM *et al*. 2021 The soundscape of the Anthropocene ocean. *Science* **371**, a4658. (doi:10.1126/science.aba4658)
5. Shabangu FW, Yemane D, Best G, Estabrook BJ. 2022 Acoustic detectability of whales amidst underwater noise off the west coast of South Africa. *Mar. Pollut. Bull*. **184**, 114122. (doi:10.1016/j.marpolbul.2022.114122)
6. Farcas A, Thompson PM, Merchant ND. 2016 Underwater noise modelling for environmental impact assessment. *Environ. Impact Assess. Rev*. **57**, 114–122. (doi:10.1016/j.eiar.2015.11.012)
7. Wenz GM. 1962 Acoustic ambient noise in the ocean: spectra and sources. *J. Acoust. Soc. Am*. **34**, 1936–1956. (doi:10.1121/1.1909155)
8. Dziak RP *et al*. 2015 Sources and levels of ambient ocean sound near the Antarctic Peninsula. *PLoS ONE* **10**, e0123425. (doi:10.1371/journal.pone.0123425)
9. Grinfeder E, Lorenzi C, Haupert S, Sueur J. 2022 What do we mean by 'soundscape'? A functional description. *Front. Ecol. Evol.* **10**, 894232. (doi:10.3389/fevo.2022.894232)

10. Payne R, Webb D. 1971 Orientation by means of long range acoustic signaling in baleen whales. *Ann. N. Y. Acad. Sci*. **188**, 110–141. (doi:10.1111/j.1749-6632.1971.tb13093.x)
11. Parks SE, Cusano DA, Stimpert AK, Weinrich MT, Friedlaender AS, Wiley DN. 2014 Evidence for acoustic communication among bottom foraging humpback whales. *Sci. Rep*. **4**, 7508. (doi:10.1038/srep07508)
12. Miller PJO, Isojunno S, Siegal E, Lam FPA, Kvadsheim PH, Curé C. 2022 Behavioral responses to predatory sounds predict sensitivity of cetaceans to anthropogenic noise within a soundscape of fear. *Proc. Natl Acad. Sci. USA* **119**, e2114932119. (doi:10.1073/pnas.2114932119)
13. Parks SE, Hamilton P, Kraus SD, Tyack PL. 2004 The 'gunshot' sound produced by male North Atlantic right whales and its potential function in reproductive advertisement. *J. Acoust. Soc. Am.* **115**, 2519–2519. (doi:10.1121/1.4783238)
14. Eichenberger F, Garland EC, Carroll EL. 2023 Reproductive tactics in baleen whales. In *Sex in cetaceans* (eds B Würsig, DN Orbach), pp. 469–498. Cham, Switzerland: Springer. (doi:10.1007/978-3-031-35651-3_20)
15. Palka DL, Hammond PS. 2001 Accounting for responsive movement in line transect estimates of abundance. *Can. J. Fish. Aquat. Sci*. **58**, 777–787. (doi:10.1139/cjfas-58-4-777)
16. Girola E, Dunlop RA, Noad MJ. 2023 Singing humpback whales respond to wind noise, but not to vessel noise. *Proc. R. Soc. B* **290**, 20230204. (doi:10.1098/rspb.2023.0204)
17. Barlow DR, Estrada Jorge M, Klinck H, Torres LG. 2022 Shaken, not stirred: blue whales show no acoustic response to earthquake events. *R. Soc. Open Sci*. **9**, 220242. (doi:10.1098/rsos.220242)
18. Republic of South Africa. 2013 Marine Living Resources, 1998 (Act No. 18 of 1998): Declaration of the Prince Edward Islands Marine Protected Area. South Africa: Department of Water and Environmental Affairs, Government Gazette No. 36575, Government Notice. 426, 13-14. See https://www.gov.za/documents/marine-living-resources-act-declaration-prince-edward-islands-marine-protected-area (accessed 4 November 2024).
19. General Bathymetric Chart of the Oceans. 2024 Gridded bathymetry data. See https://download.gebco.net/ (accessed 25 October 2024).
20. Lombard AT *et al*. 2007 Conserving pattern and process in the Southern Ocean: designing a marine protected area for the Prince Edward Islands. *Antarct. Sci*. **19**, 39–54. (doi:10.1017/s0954102007000077)
21. Rintoul SR. 2009 Antarctic Circumpolar Current. In *Encyclopedia of ocean sciences* (eds JH Steele, SA Thorpe, KK Turekian), pp. 178–190. London, UK: Academic Press. (doi:10.1016/b978-012374473-9.00603-2)
22. Reisinger RR *et al*. 2018 Habitat modelling of tracking data from multiple marine predators identifies important areas in the southern Indian Ocean. *Divers. Distrib*. **24**, 535–550. (doi:10.1111/ddi.12702)
23. Shabangu FW, Daniels R, Jordaan RK, de Bruyn PJN, van den Berg MA, Lamont T. 2024 Killer whale acoustic patterns respond to prey abundance and environmental variability around the Prince Edward Islands, Southern Ocean. *R. Soc. Open Sci*. **11**, 230903. (doi:10.1098/rsos.230903)
24. Shabangu FW *et al*. 2024 Diverse baleen whale acoustic occurrence around two sub-Antarctic islands: a tale of residents and visitors. *Sci. Rep*. **14**, 21663. (doi:10.1038/s41598-024-72696-2)
25. Tsang-Hin-Sun E, Royer JY, Leroy EC. 2015 Low-frequency sound level in the southern Indian Ocean. *J. Acoust. Soc. Am*. **138**, 3439–3446. (doi:10.1121/1.4936855)
26. Lamont T, van den Berg MA, Tutt GCO, Ansorge IJ. 2019 Impact of deep-ocean eddies and fronts on the shelf seas of a sub-Antarctic Archipelago: the Prince Edward Islands. *Cont. Shelf Res*. **177**, 1–14. (doi:10.1016/j.csr.2019.03.001)
27. Toolsee T, Lamont T. 2022 Long-term trends and interannual variability of wind forcing, surface circulation, and temperature around the Sub-Antarctic Prince Edward Islands. *Remote Sens*. **14**, 1318. (doi:10.3390/rs14061318)
28. Hijmans RJ. 2023 raster: geographic data analysis and modeling. R package version 3.6-26. See https://CRAN.R-project.org/package=raster.
29. Wickham H *et al*. 2019 Welcome to the Tidyverse. *J. Open Source Softw*. **4**, 1686. (doi:10.21105/joss.01686)
30. R Core Team. 2023 *R: a language and environment for statistical computing* (version 4.3.1). Vienna, Austria: R Foundation for Statistical Computing. See https://www.R-project.org.
31. Hersbach H, Bell B, Berrisford P *et al*. 2023 ERA5 hourly data on single levels from 1940 to present. Copernicus Climate Change Service (C3S) climate data store (CDS). See https://doi.org/10.24381/cds.adbb2d47 (accessed 3 July 2024).
32. Tournadre J, Ifremer/LOPS. 2022 Database of small icebergs from satellite altimetry for Altiberg project. Ver. 3.1. Ifremer, Plouzane, France. See https://sextant.ifremer.fr/record/06770b5a-b8aa-4a59-b66d-304c2bf9b548/ (accessed 7 November 2024).
33. Lamont T, van den Berg M. 2023 Long-term observations of hourly currents on the Prince Edward Island shelf at Mooring 1 (April 2021–May 2022). Department of Forestry, Fisheries and the Environment. See https://doi.org/10.15493/DEA.MIMS.11052023 (accessed 1 June 2024).
34. Lamont T, van den Berg M. 2023 Long-term observations of hourly currents on the Prince Edward Island shelf at Mooring 1 (May 2022–April 2023). Department of Forestry, Fisheries and the Environment. See https://doi.org/10.15493/DEA.MIMS.11152023 (accessed 1 June 2024).
35. Dugan PJ, Ponirakis DW, Zollweg JA, Pitzrick MS, Morano JL, Warde AM, Rice AN, Clark CW, Van Parijs SM. 2011 SEDNA—bioacoustic analysis toolbox. In *IEEE OCEANS'11, Waikoloa, HI, USA, 19–22 September 2011*. (doi:10.23919/oceans.2011.6107289)
36. Breiman L. 2001 Random forests. *Mach. Learn.* **45**, 5–32. (doi:10.1023/A:1010950718922)
37. Schonlau M, Zou RY. 2020 The random forest algorithm for statistical learning. *Stata J*. **20**, 3–29. (doi:10.1177/1536867x20909688)
38. Dobson AJ. 1990 *An introduction to generalized linear models*. London, UK: Chapman and Hall.
39. He H, Bai Y, Garcia EA, Li S. 2008 Adaptive synthetic sampling approach for imbalanced learning. In *Proc. 2008 IEEE Int. Joint Conf. on Neural Networks (IEEE World Congress on Computational Intelligence)*, Hong Kong, China, pp. 1322–1328. (doi:10.1109/ijcnn.2008.4633969)

40. Nallamuthu N. 2020 Handling imbalanced data: machine learning, computer vision and NLP. See https://www.analyticsvidhya.com/blog/2020/11/handling-imbalanced-data-machine-learning-computer-vision-and-nlp/ (accessed 21 October 2024).
41. Chawla NV, Bowyer KW, Hall LO, Kegelmeyer WP. 2002 SMOTE: synthetic minority over-sampling technique. *J. Artif. Intell. Res*. **16**, 321–357. (doi:10.1613/jair.953)
42. Scholbeck CA, Molnar C, Heumann C, Bischl B, Casalicchio G. 2020 Sampling, intervention, prediction, aggregation: a generalized framework for model-agnostic interpretations. In *Machine learning and knowledge discovery in databases* (eds P Cellier, K Driessens), pp. 205–216. Cham, Switzerland: Springer. (doi:10.1007/978-3-030-43823-4_18)
43. Greenwell BM, Boehmke BC, McCarthy AJ. 2018 A simple and effective model-based variable importance measure. (https://arxiv.org/abs/1805.04755)
44. Altmann A, Toloşi L, Sander O, Lengauer T. 2010 Permutation importance: a corrected feature importance measure. *Bioinformatics* **26**, 1340–1347. (doi:10.1093/bioinformatics/btq134)
45. Liaw A, Wiener M. 2002 Classification and regression by randomForest. *R News* **2**, 18–22.
46. Wright MN, Ziegler A. 2017 ranger: a fast implementation of random forests for high dimensional data in C++ and R. *J. Stat. Softw.* **77**, 1–17. (doi:10.18637/jss.v077.i01)
47. Kuhn M, Wickham H. 2020 Tidymodels: a collection of packages for modeling and machine learning using tidyverse principles. See https://www.tidymodels.org (accessed 11 December 2023).
48. McCarthy AH, Peck LS, Aldridge DC. 2022 Ship traffic connects Antarctica's fragile coasts to worldwide ecosystems. *Proc. Natl Acad. Sci. USA* **119**, e2110303118. (doi:10.1073/pnas.2110303118)
49. Shabangu FW, Branch TA, Hlati K, Samaran F, Malick I, Fennessy ST, Everett BI, van den Berg MA, Yemane D. 2025 Contraventions of MPA regulations by the South African demersal trawl fisheries: evidence from loss and damage of scientific instruments. *Reg. Stud. Mar. Sci*. **85**, 104141. (doi:10.1016/j.rsma.2025.104141)
50. Welch H, Clavelle T, White TD, Cimino MA, Van Osdel J, Hochberg T, Kroodsma D, Hazen EL. 2022 Hot spots of unseen fishing vessels. *Sci. Adv.* **8**, eabq2109. (doi:10.1126/sciadv.abq2109)
51. Shabangu F, Andrew R, Yemane D, Findlay K. 2020 Acoustic seasonality, behaviour and detection ranges of Antarctic blue and fin whales under different sea ice conditions off Antarctica. *Endanger. Species Res*. **43**, 21–37. (doi:10.3354/esr01050)
52. Menze S, Zitterbart DP, van Opzeeland I, Boebel O. 2017 The influence of sea ice, wind speed and marine mammals on Southern Ocean ambient sound. *R. Soc. Open Sci*. **4**, 160370. (doi:10.1098/rsos.160370)
53. Mattmüller RM, Thomisch K, Hoffman JI, Van Opzeeland I. 2024 Characterizing offshore polar ocean soundscapes using ecoacoustic intensity and diversity metrics. *R. Soc. Open Sci*. **11**, 231917. (doi:10.1098/rsos.231917)
54. Shabangu FW, Yemane D, Stafford KM, Ensor P, Findlay KP. 2017 Modelling the effects of environmental conditions on the acoustic occurrence and behaviour of Antarctic blue whales. *PLoS ONE* **12**, e0172705. (doi:10.1371/journal.pone.0172705)
55. Shabangu FW, Findlay KP, Yemane D, Stafford KM, van den Berg M, Blows B, Andrew RK. 2019 Seasonal occurrence and diel calling behaviour of Antarctic blue whales and fin whales in relation to environmental conditions off the west coast of South Africa. *J. Mar. Syst*. **190**, 25–39. (doi:10.1016/j.jmarsys.2018.11.002)
56. Matsumoto H, Bohnenstiehl DR, Tournadre J, Dziak RP, Haxel JH, Lau T -K. A, Fowler M, Salo SA. 2014 Antarctic icebergs: a significant natural ocean sound source in the Southern Hemisphere. *Geochem. Geophys. Geosystems* **15**, 3448–3458. (doi:10.1002/2014gc005454)
57. Amron A, Alam FC, Trenggono M, Hidayat RR, Nur Meinita MD. 2020 Noise characteristics of sea waves based on its height, period and breaking waves. *J. Phys*. **5**, 28–34. (doi:10.22437/jop.v5i2.9509)
58. Lurton X, Cuschieri JM. 2011 An introduction to underwater acoustics—principles and applications (second edition). *Noise Control Eng. J*. **59**, 106. (doi:10.3397/1.3525563)
59. Gao Y, Schmitt FG, Hu J, Huang Y. 2023 Probability-based wind-wave relation. *Front. Mar. Sci*. **9**, 1085340. (doi:10.3389/fmars.2022.1085340)
60. Hildebrand J. 2009 Anthropogenic and natural sources of ambient noise in the ocean. *Mar. Ecol. Prog. Ser*. **395**, 5–20. (doi:10.3354/meps08353)
61. Haver SM, Klinck H, Nieukirk SL, Matsumoto H, Dziak RP, Miksis-Olds JL. 2017 The not-so-silent world: measuring Arctic, equatorial, and Antarctic soundscapes in the Atlantic Ocean. *Deep Sea Res. Part I* **122**, 95–104. (doi:10.1016/j.dsr.2017.03.002)
62. van den Hoff J, Delarue J, Warren V, McPherson C, Lieser J, Achurch H, Virtue P, Miller B. 2025 Origins of natural and anthropogenic sounds in a coastal, seasonally ice-covered, Antarctic marine soundscape. *Mar. Ecol. Prog. Ser*. **757**, 17–36. (doi:10.3354/meps14813)
63. Zheng CW, Pan J, Li CY. 2016 Global oceanic wind speed trends. *Ocean Coast. Manag*. **129**, 15–24. (doi:10.1016/j.ocecoaman.2016.05.001)
64. Shabangu FW, Ona E, Yemane D. 2014 Measurements of acoustic attenuation at 38 kHz by wind-induced air bubbles with suggested correction factors for hull-mounted transducers. *Fish. Res*. **151**, 47–56. (doi:10.1016/j.fishres.2013.12.008)
65. Shabangu FW, Yemane D, Stander N, Estabrook BJ. 2025 Underwater soundscape indicates low anthropogenic influence around two sub-Antarctic islands. Dryad. (doi:10.5061/dryad.9s4mw6mtf)
66. Shabangu FW, Yemane D, Stander N, Estabrook BJ. 2025 Supplementary material from: Underwater soundscape indicates low anthropogenic influence around two sub-Antarctic islands. Figshare. (doi:10.6084/m9.figshare.c.8151827)